Proceedings of the IASTED International Conference
Modelling and Simulation (AfricaMS 2012)
September 3 - 5, 2012 Botswana, Africa

FORWARD AND REVERSE MIDDLE EAR FREQUENCY RESPONSES WITH VARIOUS TERMINAL LOADS

Tshegofatso Thejane
CSIR-Modelling and Digital Sciences,
Pretoria, South Africa
and University of Johannesburg,
Johannesburg, South Africa
Email: tthejane@csir.co.za

Tshilidzi Marwala
Faculty of Engineering and
the Built Environment,
University of Johannesburg,
Johannesburg, South Africa

Jacoba E. Smit and Fulufhelo V. Nelwamondo
CSIR-Modelling and Digital Sciences,
Pretoria, South Africa

ABSTRACT
An analog network model of the human middle ear is used to study the effect of terminal loads on the middle ear frequency response. A new transformer ratio value is computed and used to improve the model of the middle ear through the use of an ideal transformer. The terminal loads are taken as the loads on either side of the middle ear. The forward and reverse frequency characteristics of the middle ear are computed using various cochlear and outer ear impedances as the terminal load, respectively. The cochlear loads used are an open circuit, a resistive load and an RCL load. The outer ear loads used are an open circuit, a outer ear transmission line model having a constant auditory canal radius and an outer ear transmission line model having a varying auditory canal radius. The components of the cochlear and outer ear loads are computed using previously published anatomical data. The RCL load proved to give the most accurate response for the forward frequency response whereas the open circuit response proved to be the most accurate for the reverse frequency response. The outer ear load models used give minimal accuracy as terminal loads and should thus be improved.

KEY WORDS
Analog network, cochlea, frequency response, load, middle ear, transformer ratio.

1. Introduction

Hearing loss is a prevalent sensory impairment. Conductive hearing loss, which often results from external or middle ear disorders, can be better treated through a in depth understanding of the mechanics of the hearing organ [1]. Middle ear modelling and simulation is one of the techniques which assist in the advancement of surgical reconstruction techniques and implantable hearing devices [1]; which are both important for hearing loss treatment. The main purpose of the middle ear is to transmit incident sound waves from the outer ear to the inner ear; where they are interpreted. Since sound travels through an air medium in the outer ear to a liquid medium in the inner ear, transmitting the sound signal directly from the outer ear to the inner ear without any impedance match will result in significant loss in its amplitude. The middle ear thus acts as an impedance matcher.

The effective transmission of sound from the outer ear to the inner ear, and hearing in general, is greatly dependent on the well-being of the middle ear. Physically measuring the transfer function of the middle ear usually requires invasive methods. A middle ear model enables for the characteristics of the middle ear to be studied without damaging any part of the ear [2]. The transfer function of the middle ear can be computed using mathematical functions. However, mathematical representation does not adequately describe the behavior of each auditory organ, but only gives a global view of their functions [2]. When using electroacoustic principles, the factors representing the middle ear physical phenomena, such as viscous losses, heat conduction, mass and elasticity of the organs, can be modeled using electrical components [2]. In electroacoustic analogy voltage represents pressure, current represents volumetric flow, inductance represents mass, capacitance represents compliance and electric resistance represents acoustic resistance [3].

Empirical research into the middle ear began over four and a half centuries ago [4], [5] and since then, interest into middle ear dynamics has risen rapidly. An analog network derived by Zwislocki in 1962 [5], which is now widely used, serves as a significant step in the development of a quantitative theory of middle ear acoustics. The middle ear model research focus was mainly in gaining understanding into the functional anatomy and pathology of the middle ear. It was not until the discovery of otoacoustic emissions (OAEs) by Kemp in 1978 [6] that the influence of the middle ear on OAEs became of interest.

Although most interest in middle ear studies are centered around middle ear pathology for sound transmission and perception, the influence of the middle ear in OAE

DOI: 10.2316/P.2012.761-026

measurements is also significant [7], [8]. OAEs are small signals generated in the inner ear and recorded in the outer ear by means of a microphone [9]. Since the OAEs pass through the middle ear before being recorded in the outer ear, being able to acquire decent OAE signals depends greatly on the condition of the middle ear. Some OAEs are spontaneously generated (Spontaneous Otoacoustic Emissions (SOAEs)) whilst other OAEs are evoked by means of a stimulus (Transient Evoked Otoacoustic Emissions (TEOAEs) and Distortion Product Otoacoustic Emissions (DPOAEs)). A pathological middle ear may not allow for a large enough stimulus to pass through and evoke OAEs or it would inhibit the transmission of OAEs. It is difficult to detect evoked OAEs in the presence of significant hearing loss [10]. It is important for sound transmission through the middle ear to be normal in both propagation directions, namely the forward direction for sending the stimuli and the reverse direction for detecting the OAE response in the ear canal. The condition of the middle ear is determined through the use of a tympanogram [11]. This study focuses only on non-pathological conditions of the middle ear.

Various studies have been conducted to investigate the influence of the middle ear on OAEs. These studies, which include [12], [7], [10], [13], do not consider the influence of the middle ear on OAEs for biometric applications. A study was conducted by Swabey et al. [14] which investigates the biometric potential of TEOAEs. Swabey et al. [14] found that there is a high level of classification that can be obtained using raw time data without transformation. This gives the indication that TEOAEs have some potential of being used as a biometric [9].

This paper aims to: (1) improve the middle ear model by computing a new transformer ratio, (2) compute the forward middle ear frequency response with various cochlear loads and (3) compute the reverse middle ear frequency response with various outer ear loads. The paper is structured as follows: the middle ear model and terminal loads are described in Section 2, the results are given and a discussion in Section 3 and 4, respectively. The paper is concluded in Section 5.

2. Model

2.1 Middle Ear Model

The middle ear is made up of the tympanic membrane, the ossicular chain (malleus, incus and stapes), the ligaments and tendons which suspend the ossicular chain and the bony cavity. The middle ear functionality can be represented using five blocks as identified in [5]. These blocks, in order of sequence of forward middle ear signal transmission, are the middle ear cavities, the eardrum motion (which is independent of the ossicular chain), the ossicular chain and eardrum movement (which is coupled with the ossicular chain movement), the incudo-stapedial chain energy losses and lastly, the stapes motion with the oval window, the impedance of the cochlea and the round window membrane (not shown on Figure 1). The middle ear cavities' functional block precedes the eardrum motion block because any displacement of the eardrum is reflected in the compression/expansion of the middle ear cavities, although this movement may not be significant enough to displace the ossicular chain [5].

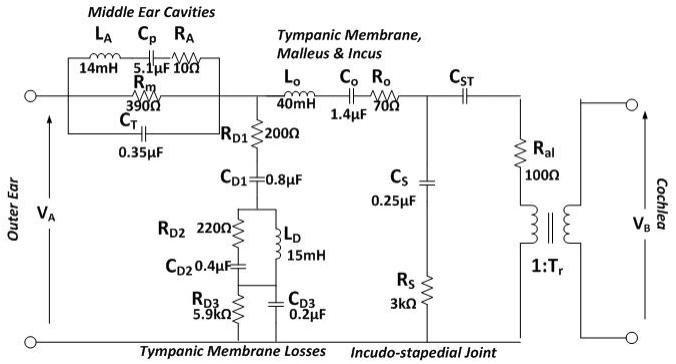

Figure 1. Middle ear analog model (as adapted from [10])

An ideal transformer is used to represent the linear amplification effect of the middle ear as shown on Figure 1. The transformer ratio T_r is defined as [2]:

$$T_r = R_l R_a \tag{1}$$

where R_l is the lever ratio (defined as the length of the long process of the incus to the length of the manubrium) and R_a is the area ratio (defined as the ratio of the area of the tympanic membrane to the area of the stapes footplate). Zhao et al. [15] conducted a review of the middle ear transfer function and collected middle ear dimension values from various researchers. Using the average of the values provided by Wever and Lawrence [16], Sun et al. [1], Koike et al. [17], Gan et al. [18] and Lee et al. [19], the average area and lever ratios are 19.57 and 1.42, respectively. This lever ratio and area ratio value gives a transformer ratio T_r of 27.79 and thus a gain of 28.88 dB. This transformer ratio is close to that of 28 dB found in [20].

There are two mechanisms which result in a nonlinear response of the middle ear, namely the stapedius muscle action and the stapes clipping displacement [2]. The stapedius muscle action is activated above 80 dB by the contraction of the stapedius muscle and stapes clipping displacement is activated above 120 dB by the clipping displacement of the stapes [2]. OAE evoking signals and their responses have small amplitudes [9]. Since the stapedius muscle action and stapes clipping displacement are activated at 80 dB and 120 dB, respectively, they will not be active during the transmission of OAEs. This is supported by Zheng et al. [21] where the stapedius muscle action is omitted when simulating TEOAEs. A Standard Pressure Level (SPL) dependant variable capacitance and resistance are generally used to represent the acoustic reflex action and the annular ligament effects [2] in analog electrical

circuits. These components have been excluded from the model in Figure 1 since the study focuses on OAEs.

2.2 Cochlear Impedance Load

The cochlear input impedance is used as the middle ear load for the forward direction. Three cochlear loads were computed for the study namely, no load, a resistive load and an RCL load. The no load condition was achieved by setting the secondary terminals of the transformer to an open circuit.

Although the cochlea, like any acoustic system, has a compliance, mass and resistance, its properties are argued to exhibit mostly a resistive behavior [2]. According to measurements conducted by [22], the resistivity of the cochlear wall varies between 546-643 Ωm, thus giving an average resistivity of 594.5 Ωm. Using this gerbil cochlear resistivity value together with the mean length of 33.31 mm of the Organ of Corti found in [23], the cochlear resistance is 17.85 kΩ.

The last cochlear load is represented by a series combination of a capacitor C, inductor L and resistor R. The capacitor represents compliance, the inductor represents mass and the resistor represents resistance of the cochlea. The cochlear impedance used is computed from the load given by Zwislocki [5]. Since an ideal transformer is used in this study, the equivalent cochlear load for the secondary side of the transformer should be computed.

This transformation was computed using the following equation:

$$Z_{secondary} = Z_{primary} {T_r}^2 \tag{2}$$

A transformation of the cochlear impedance Z of $R + j\omega L + (j\omega C)^{-1}$ using (2) results in the following modifications to the cochlear load impedance component values:

$$R_{new} = R{T_r}^2 \tag{3}$$

and

$$L_{new} = L{T_r}^2 \tag{4}$$

and

$$C_{new} = \frac{C}{{T_r}^2} \tag{5}$$

Using the transformer ratio given in [5] of 22, the resulting cochlear load as seen on the secondary side of the transformer is made up of the component values 290.4 kΩ, 9.63 H and 1.23 nF for the resistor, inductor and capacitor, respectively.

2.3 Outer Ear Impedance Load

The outer ear impedance is used as the middle ear load for the reverse direction. Three outer ear loads were computed for the study namely, no load, a load computed from a constant auditory canal radius and a load computed from a varying auditory canal radius. The no load condition was achieved by setting the terminal V_A to an open circuit.

The outer ear model is composed of the external ear, the concha and the auditory canal as shown on Figure 2. L-segment and M-segment transmission line models have been used to represent the concha and auditory canal, respectively.

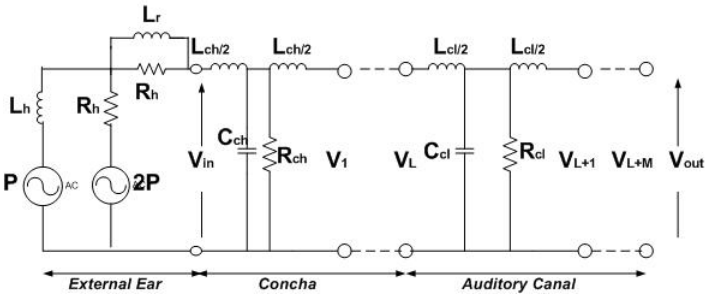

Figure 2. Outer ear circuit model (reproduced from [24]). The circuit serves as a load to the middle ear for propagation in the reverse direction [24]. The component values are calculated as outlined in [24].

The component values of the above model were calculated using the equations given in Giguere and Woodland's study [3]. Of these equations, the M segment auditory canal components are given by the following relationships [3]:

$$Inductance = \frac{\rho_a \Delta x}{\pi a^2} \tag{6}$$

and

$$Capacitance = \frac{\pi a^2 \Delta x}{\rho_a c^2} \tag{7}$$

and

$$Resistance = \frac{2\alpha \Delta x}{Z} \tag{8}$$

where ρ_a is the density of air, Δx is the segment length of the transmission line, a is the radius of the auditory canal, c is the velocity of sound, α is the effective attenuation constant and Z is the characteristic impedance given by $\sqrt{\frac{Inductance}{Capacitance}}$.

For the case of the outer ear load computed using a constant radius of the auditory canal, the radius value 3.5 mm [3] was used. For the case where the outer ear load computed using a varying radius of the auditory canal, we computed a radius-length mapping function for the auditory canal in a previous study [24]. This function was used to approximate the manner in which the auditory canal varies along its length, whereas previous studies have incorrectly assumed a uniform radius [24]. Figure 3 illustrates the two polynomials making up the radius-length mapping function.

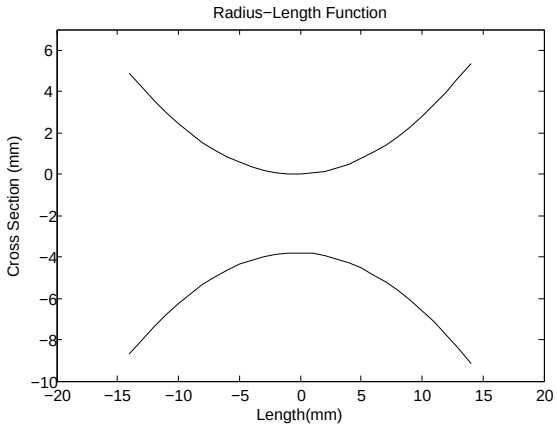

Figure 3. Radius-length mapping function (reproduced from [24])

The radius of the auditory canal is calculated as the absolute value of the difference between the following polynomials [24]:

$$y_1 = 0.026x^2 + 0.016x \tag{9}$$

and

$$y_2 = -0.026x^2 - 0.016x - 0.379 \tag{10}$$

where x is a point along the length of the auditory canal and y_1 and y_2 are the upper and lower curves of the auditory canal at that point x as shown on Figure 3. For all load cases of the reverse middle ear transfer function, it is assumed that no input signal is coming from the entrance of the outer ear. This is achieved by short circuiting the voltage sources P and $2P$ illustrated in Figure 2 to zero. Contrary to other models, this outer ear model includes the effect of the head, pinna and concha in the outer ear model. This is particularly significant for the study since these parts (head, pinna and concha) would be influential if the model was to be used in the study of the biometric potential of OAEs [9], [24] (i.e. with the cellphone being the source of stimulus). A small resistor of 0.01 $m\Omega$ is also inserted in series with the secondary terminals of the transformer and the intracochlear voltage source placed at V_B to allow for an ideal voltage source to be used as the intracochlear source.

3. Results

The transfer function of a system is the ratio of the system's output to its input [25]. The transfer function allows for the frequency response of the middle ear to be characterized and hence its effect on OAEs to be simulated. Since a frequency response is the graphical realization of a transfer function, frequency response plots are used in this study.

An intracochlear sound source is usually required for obtaining the reverse transmission characteristics of the middle ear. This is usually accomplished by using two pure tones of frequencies f_1 and f_2 in various combinations such $2f_1 - f_2$ and $2f_2 - f_1$ [12]. These combinations are termed Distortion Products (DPs) and they are generally used to induce DPOAEs [11]. In this study, the frequency response of the middle ear is studied by means of bode plots.This eliminates the need to alter the DP frequencies and conduct various simulations.

Most OAEs have a frequency range in the span of kilohertz (kHz). Dong and Olson [12] conducted a study on measuring the forward and reverse transmission characteristics of the middle ear in gerbil. Their measurements revealed that the highest frequency for which both DPs and DPOAEs could be detected was between 20-30 kHz. Although this range may be different for humans, it is used as a starting point for the range of interest of the study.

3.1 Forward Middle Ear Frequency Response

The forward middle ear transfer function is defined as the ratio of the intracochlear voltage V_B to the tympanic membrane voltage V_A as labeled in Figure 1. The outer ear is not expected to act as a load in the forward transmission, thus only the cochlear model is used as a load in this case.

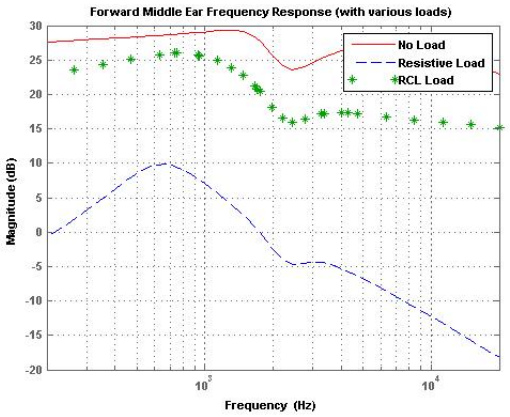

Figure 4. Forward Middle Ear Frequency Response (Magnitude)

Figure 4 gives the magnitude component of the middle ear forward frequency response. There are various ways of observing the frequency characteristics of the middle ear, the most common of which is to use a laser Doppler measuring system (LDS). The LDS measures the displacement of the umbo, malleus and stapes from which the transfer function is computed. A different measurement technique which uses a sweeping stimulus frequency to measure the middle ear dynamic characteristics under physiological conditions was used in [8]. This technique revealed that the resonance frequency of the middle ear in subjects

with normal hearing is around 1.17 kHz [8]. This result is also supported by Goode et al. [26] and Nobili et al. [27] who both found that the pressure gain maximum value is around 1000 Hz. As expected, the response for the no load case gives the highest gain for wide range of frequencies. This gain is however to high for average peak gain of about 20 dB around 1 kHz as measured by Puria [13]. The magnitude response obtained when using an RCL load corresponds the closest the responses measured by Puria [13]. The response obtained when using a purely resistive load gives a peak gain of about 10 dB. The resonant frequency obtained for this peak gain is less than 1 kHz; which is not within the expected range.

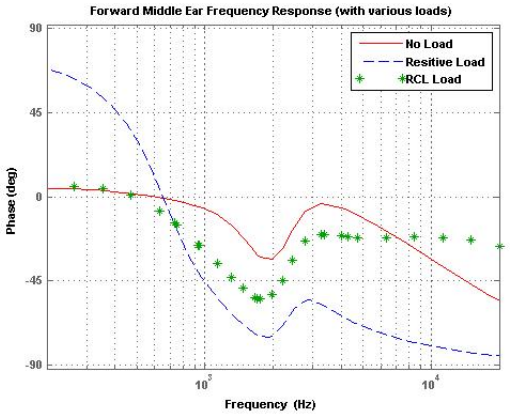

Figure 5. Forward Middle Ear Frequency Response (Phase)

The corresponding phase frequency plot is found above in Figure 5. The response obtained for an RCL load gives the closest response to measured values, whereas the response obtained when using the resistive load is the farthest from measurements.

3.2 Reverse Middle Ear Frequency Response

The reverse middle ear transfer function is defined as the ratio of the tympanic membrane voltage V_A to the intracochlear voltage V_B [2] as labeled in Figure 1. The cochlear load impedance does not affect the reverse transfer function and is thus omitted.

Figure 6 gives the magnitude component of the middle ear reverse frequency response. Not much work has been conducted on the reverse frequency characteristics of the middle ear. Nobili et al. [27] found a frequency response similar in shape to the one for the forward direction transfer function with a peak pressure gain of -30 dB at 1000 Hz [27]. Similarly, a peak gain of -30 dB around 1.5 kHz was found from measurements conducted by Puria [13]. The peak value for the responses with the loading is mostly below -60 dB. Although the first peak is close to 1000 Hz, its magnitude is far off from the expected first peak value of -30 dB as measured by Nobili et al. [27] and

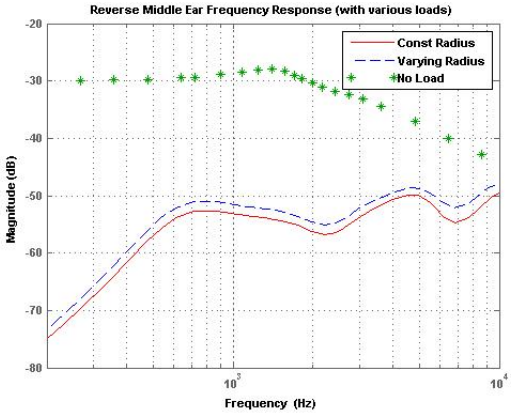

Figure 6. Reverse Middle Ear Frequency Response (Magnitude)

Puria [13]. The gain is also expected to exhibit a steady decline for the frequency range above the first peak frequency as measured by both Nobili et al. [27] and Puria [13]. It can be seen from Figure 6 that of the three responses, the response for the case with zero load exhibits the closest behavior. The responses for the two loads (i.e. constant radius and varying radius) have a similar shape through most of the frequencies, except a shift in the gain and an incline in the gain for frequencies above -30 dB.

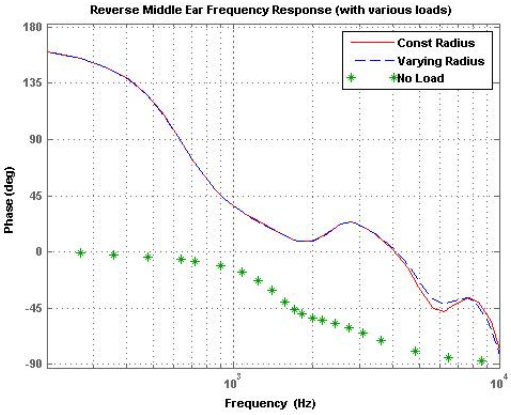

Figure 7. Reverse Middle Ear Frequency Response (Phase)

The corresponding phase frequency plot is found above in Figure 7. Again, the response obtained from the measurements conducted by Puria [13] correspond more closely with the response obtained when having no load with the peak phase for both responses being slightly above zero degrees.

4. Discussion

Although a constant lever ratio was used for the calculation of the transformer ratio, an experiment conducted on temporal bones shows that there is a difference in the slopes of the umbo and stapes vibration above 1000 Hz such that an increase in the ratio occurs with a rise in frequency [26]. This variation in the vibration is argued to be due to a slippage in the ossicular system at higher frequencies [26] and should thus be considered in later studies. The outer ear load was computed under the assumption that there is not interfering signal from the outer ear. This model, alone, is thus not suitable for the study of the biometric application of OAEs since the transceiver is already outside the auditory canal and is thus prone to noise. A model which accounts for the typical noise signals received during the use of potential OAE biometric transceivers (e.g. cellphones) should be computed.

Both the magnitude and phase plots of the reverse middle ear frequency response show that the response which corresponds with measurements is the one obtained when there is no load on the outer ear terminal of the middle ear. Although part of the difference between the responses with a load and one without a load can be accounted for by the fact that the the outer ear loads used in the study incorporate the outmost model of the outer ear (i.e. head and pinna), whereas measurements are conducted without taking them into consideration, the responses obtained under loading conditions is still far off from the expected range. It can thus be argued that the model does not sufficiently represent the outer ear load and should thus be improved. Part of the improvement can stem from refining the radius length function of the auditory canal to include a three dimensional representation of the radius-length relationship and not just the two dimensional view as shown on Figure 3. All responses show a negative gradient for the reverse phase frequency relationship. This negative slope corresponds to an expected time delay in the OAEs frequency components demonstrated by Zheng et al. [21] from the decomposition of TEOAEs from a similar analog model , only more comprehensive (i.e. the action of the outer hair cells are included).

5. Conclusion

The frequency characteristics of the middle ear have been studied for both forward and reverse transmission direction using various terminal loads. The forward middle ear response shows that the resistive load, alone, does give the desired frequency response shape. Although the resistance dominates the load impedance of the cochlear, inductive and capacitive components are also required to give a more accurate representation of the cochlear load. The outer ear load has proved to need further improvement in order to give the expected reverse transmission frequency characteristics. The combined forward and reverse middle ear frequency responses showed that although the middle ear acts as an impedance matcher, there is still a significant amplitude reduction in the reverse transmission direction and thus an efficient mechanism of acquiring and processing OAEs is required.

Acknowlegements

The authors wish to thank the CSIR for its resources and their colleagues for their support during the compilation of this paper.

References

[1] Q. Sun, R. Z. Gan, K. H. Chang, and K. J. Dormer, "Computer-integrated finite element modelling of human middle ear," *Biomechan Model Mechannobiol*, 2002.

[2] J. Pascal, A. Bourgeade, M. Lagier, and C. Legros, "Linear and nonlinear model of the human middle ear," *J. Acoust. Soc. Am.*, vol. 104, no. 3, pp. 1509–1516, 1998.

[3] C. Giguere and P. C. Woodland, "A computational model of the auditory periphery for speech and hearing research. i. ascending path," *J. Acoust. Soc. Am.*, vol. 95, pp. 331–342, 1994.

[4] G. von Bekesy and W. A. Rosenblith, "The early history of hearing-observations and theories," *J.Acoust. Soc. Am.*, vol. 34, pp. 1514–1523, 1948.

[5] J. Zwislocki, "Analysis of the middle ear function. part i. input impedance," *J.Acoust. Soc. Am.*, vol. 34, 1962.

[6] D. T. Kemp, "Simulated acoustic emissions from within the human auditory system," *J. Acoust. Soc. Am.*, vol. 64, pp. 1386–1391, 1978.

[7] Y. Salimpour and M. D. Abolhassani, "Reverse middle ear transfer function based estimation of transient evoked otoacoustic emission," in *Proceedings of the 4th IEEE-EMBS International Summer School and Symposium on Medical Devices and Biosensors*, St Catharine's College, 2007, pp. 82–85.

[8] F. Zhao, H. Wada, T. Koike, and D. Stephens, "The influence of middle ear disorders on otoacoustic emissions," *Clin. Otolaryngol*, vol. 25, pp. 3–8, 2000.

[9] T. Thejane, F. V. Nelwamondo, T. C. Malumedzha, and T. Marwala, "Otoacoustic emissions: A review on exisiting human auditory system modelling approaches," in *Proceedings of the IASTED International Conference on Modelling and Simulation (MS 2011)*, Calgary, Canada, 2011.

[10] P. Avan, B. Buki, B. Maat, D. M., and H. P. Wit, "Middle ear influence on otoacoustic emissions. i: Noninvasive investigation of the human transmission apparatus and comparison with model results," *Hearing Research*, vol. 140, 1999.

[11] M. S. Robinette and T. J. Glattke, *Otoacoustic Emissions: Clinical Applications*. New York, USA: Thieme Medical Publishers, 2007.

[12] W. Dong and E. S. Olson, "Middle ear forward and reverse transmission in gerbil," *JN Physiol*, vol. 95, pp. 2951–2961, 2006.

[13] S. Puria, "Measurements of human middle ear ear forward and reverse acoustics: Implications for otoacoustic emissions," *J. Acoust. Soc. Am.*, vol. 113, pp. 2773–2789, 2003.

[14] M. S. Swabey, P. Chambers, M. E. Lutman, N. M. White, J. E. Chad, A. D. Brown, and S. P. Beeby, "The biometric potential of transient evoked otoacoustic emissions," *Int. J. of Biometrics*, vol. 1, pp. 349–364, 2009.

[15] F. Zhao, T. Koike, J. Wang, H. Sienz, and R. Meredith, "Finite element analysis of the middle ear transfer functions and related pathologies," *Med. Eng. and Phys.*, vol. 31, pp. 907–916, 2009.

[16] E. G. Wever and M. Lawrence, *Physiological Acoustics*. Princeton: Princeton University Press, 1982.

[17] T. Koike, H. Wada, and T. Kobayashi, "Modelling of the human middle ear using the finite-element method," *J. Acoust. Soc. Am.*, vol. 111, pp. 1306–1317, 2002.

[18] R. Z. Gan, B. Feng, and Q. Sun, "Three-dimensional finite element modelling of human ear for sound transmission," *Ann. Biomed. Eng.*, vol. 32, pp. 847–859, 2004.

[19] C. F. Lee, P. R. Chen, W. J. Lee, J. H. Chen, and T. C. Liu, "Three-dimensional reconstruction and modelling of middle ear biomechanics by high-resolution computed tomography and finite element analysis," *Laryngoscope*, vol. 116, pp. 711–716, 2006.

[20] A. J. Guyla, L. B. Minor, and D. S. Poe, *Glasscock-Shambaugh's Surgery of the Ear*, 6th ed. USA: People's Medical Publishing Home, 2010.

[21] L. Zheng, Y. T. Zhang, F. S. Yang, and D. T. Ye, "Synthesis and decomposition of transient-evoked otoacoustic emissions based on an active auditory model," *IEEE Transactions on Biomedical Engineering*, vol. 46, pp. 1098–1106, 1999.

[22] G. Kumar, M. Chokshi, and C.-P. Richter, "Electrical impedance measurements of cochlear structures using the four-electrode reflection-coefficient technique," *Hearing Research*, vol. 259, pp. 86–94, 2010.

[23] D. Sridhar, O. Stakhovskaya, and P. A. Leake, "A frequency-position function for the human cochlear spiral ganglion," *Audiol Neurootol*, vol. 11, pp. 16–20, 2006.

[24] T. Thejane, F. V. Nelwamondo, J. E. Smit, and T. Marwala, "Influence of the auditory canal number of segments and radius variation on the outer ear frequency response," in *Proceedings of the IEEE-EMBS International Conference on Biomedical and Health Informatics (BHI 2012)*, Hong Kong and Shenzhen, China, 2012, pp. 384–387.

[25] R. S. Burns, *Advanced Control Engineering*. Oxford, UK: Butterworth-Heinemann Publishers, 2001.

[26] R. L. Goode, M. Killion, K. Nakamura, and S. Nishihara, "New knowledge about the function of the human middle ear: Development of an improved analog model," *The American Journ of Otology*, vol. 15, no. 2, pp. 145–154, 1994.

[27] R. Nobili, A. Vetesnik, L. Turicchia, and F. Mammano, "Otoacoustic emissions from residual oscillations of the cochlear basilar membrane in a human ear model," *JARO*, vol. 4, pp. 478–494, 2003.